3rd Symposium on Lift and Escalator Technologies

# Modeling and simulation of a high-rise elevator system to predict the dynamic interactions between its components

Rafael Sánchez Crespo[1], Stefan Kaczmarczyk[1], Phil Picton[1], Huijuan Su[1], and Markus Jetter[2]

[1] School of Science and Technology, The University of Northampton, U.K.

[2] ThyssenKrupp Elevator AG, CoRE - Center of Research Europe, Germany

## ABSTRACT

Lateral vibrations of suspension and compensating ropes in a high-rise elevator system are induced by the building motions. When the frequency of the building coincides with the fundamental natural frequency of the ropes, large resonance whirling motions of the ropes result. This phenomenon leads to impacts of the ropes the elevator walls, making the building and elevator system unsafe. The impact loads affect the performance of the elevator installation resulting in interruptions of service and damage to the components of the system. Furthermore, the car, counterweight and compensating sheave suffer from vertical vibrations due to the coupling with the lateral vibrations of the ropes. This paper presents a comprehensive mathematical model of a high-rise elevator system taking into account a scenario when the car is parked at the landing level corresponding to the resonance length of the ropes. The model is implemented in a high performance computational environment and the dynamic response of the system when the building is subject to a low frequency sway, is determined through numerical simulation. The results predict a range of nonlinear dynamic interactions between the components of the elevator system that play a significant role in the operation of the entire installation.

## INTRODUCTION

Lateral vibrations of the suspension and compensating ropes in a high-rise elevator system are induced by the building motions caused by high winds in the in-plane and the out of plane directions. When one of the two fundamental frequencies of the building coincides with one of the natural frequencies of the ropes, large resonance whirling motions of the ropes result. This phenomenon results in impact loads in the elevator shaft, leading to adverse dynamic behavior of the elevator system. The impact loads affect the elevator installation resulting in interruptions of service and damage to the components of the system. Furthermore, the car, counterweight and compensating sheave suffer from vertical vibrations due to the coupling with lateral vibrations of the ropes.

The behavior of a suspension rope – elevator car system was studied in [1,2]. The study involved a suspension rope of time-varying length with a mass representing an elevator car traveling according to a prescribed velocity and acceleration time-profiles. The excitation was implemented though harmonic motions applied at the top of the hoist structure. Autoparametric nonlinear nonstationary resonance phenomena were then investigated through a range of numerical simulation test.

This paper presents a comprehensive mathematical model of a high-rise stationary elevator system taking into account a scenario when the car is parked at the landing level corresponding to the resonance length of the compensating ropes. The model is implemented in the MATLAB computational environment and the dynamic response of the system when the building is subjected

to a low frequency sway in both lateral in-plane and lateral out-plane, is determined using numerical simulation techniques. The results predict a range of nonlinear dynamic interactions between the components of the elevator system that play a significant role in the operation of the entire installation.

## DESCRIPTION OF THE MODEL OF AN ELEVATOR SYSTEM

The elevator ropes are flexible and have low internal damping. Therefore, at resonance conditions they often vibrate at large amplitudes.

The model of an elevator system with a car of mass $M_1$, compensating sheave of mass $M_2$, and counterweight of mass $M_3$, is depicted in Fig. 1. The suspension and compensating ropes have mass per unit length $m_1$ and $m_2$, elastic modulus $E_1$ and $E_2$, and effective cross-section are $A_1$ and $A_2$, respectively. The parameter $b_1$ represents the distance measured from the bottom landing level to the center of the compensating sheave. The parameter $b_2$ denotes the distance measured from the center of the traction sheave to the center of the diverter pulley and $h_0$ represents the distance measured from the bottom landing level to the center of the traction sheave. The parameter $h_{trav}$ is the height of travel of the elevator car. The parameter $h_{car}$ is the height of the car. The parameter $h_{cw}$ is the height of the counterweight. The parameter $h_t$ is the position of the elevator car measured from the bottom landing level to the bottom of the elevator car.

The lengths of the suspension rope and of the compensating rope are defined as follows. The length of the suspension rope at the car side measured from the center of the traction sheave to the the termination at the car crosshead beam is denoted by $L_1$. The length of the compensating rope at the car side measured from the termination at the car bottom to the center of the compensating sheave is denoted as $L_2$. The length of the compensating rope at the counterweight side measured from the termination at the counterweight to the center of the compensating sheave is denoted by $L_3$. The length of the suspension rope at the counterweight side measured from the center of the diverter pulley to the termination at the counterweight end is denoted by $L_4$. The mass moment of inertia of the diverter pulley and the short stretch of the suspension rope between the pulley and the traction sheave is neglected in the simulation model.

The response of the elevator ropes subjected to dynamic loading due to the building sway are represented by the lateral in-plane and lateral out of plane displacements denoted as $V_i(x_i,t)$ and $W_i(x_i,t)$ where the subscript $i=1,2,3,4$ corresponds to the sections of the ropes of length $L_1$, $L_2$, $L_3$, and $L_4$, respectively. The lateral in-plane and lateral out of plane motions of the ropes are coupled with the longitudinal motions of the ropes that are denoted as $U_i(x_i,t)$. The longitudinal motions of the car, compensating sheave and counterweight are denoted as $U_{CR}(t)$, $U_{CS}(t)$, and $U_{CW}(t)$, respectively.

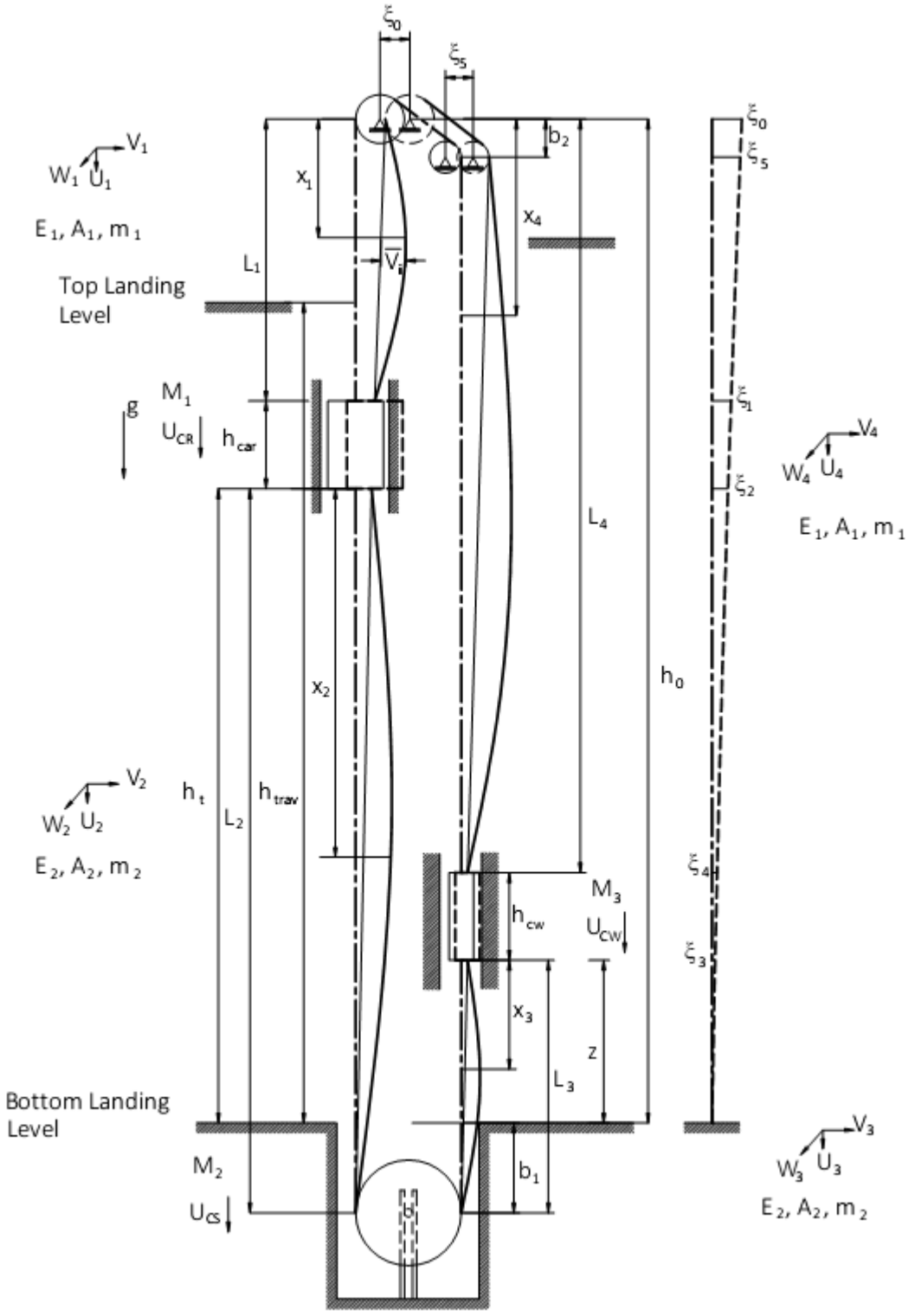


Figure 1. Elevator system.

The building structure is subjected to bending deformations in the in-plane and out of plane directions, described by the shape function $\Psi(z)$, with z denoting a coordinate measured from the bottom landing level. The bending deformations result in harmonic motions $C_v(t)$ and $C_w(t)$ of frequency $\Omega_v$ and $\Omega_w$ and amplitude $A_v$ and $A_w$ in the lateral in-plane and lateral out of plane directions, respectively.

**VIBRATION MODEL**

The mean tensions of each stretch of the ropes are expressed as

$$T_1(x_1) = M_1 g + m_1 g\left(L_1 - x_1\right) + m_2 g L_2 + \frac{M_2 g}{2}. \tag{1}$$

$$T_2(x_2) = \frac{M_2 g}{2} + m_2 g\left(L_2 - x_2\right). \tag{2}$$

$$T_3(x_3) = \frac{M_2 g}{2} + m_2 g\left(L_3 - x_3\right). \tag{3}$$

$$T_4(x_4) = M_3 g + m_1 g\left(L_4 - x_4\right) + m_2 g L_3 + \frac{M_2 g}{2}. \tag{4}$$

where g is the acceleration of gravity and $x_i$ represent the spatial coordinate corresponding to the sections of the ropes of length $L_1$, $L_2$, $L_3$, and $L_4$, respectively. The axial Green's strain measure representing stretching of the rope section $i$ is given as

$$\varepsilon_i = U_{ix} + \frac{1}{2}\left(V_{ix}^{\ 2} + W_{ix}^{\ 2}\right). \tag{5}$$

where $\left(\ \right)_x \equiv \frac{\partial(\ )}{\partial x}$ . The equations governing the undamped dynamic displacements $U_i(x_i,t)$, $V_i(x_i,t)$, $W_i(x_i,t)$, $U_{CR}(t)$, $U_{CS}(t)$, and $U_{CW}(t)$ can be developed by applying Hamilton's principle, which yields

$$m_i V_{itt} - T_{ix} V_{ix} - E_j A_j \varepsilon_{ix} V_{ix} - T_i V_{ixx} - E_j A_j \varepsilon_i V_{ixx} = 0. \tag{6}$$

$$m_i W_{itt} - T_{ix} W_{ix} - E_j A_j \varepsilon_{ix} W_{ix} - T_i W_{ixx} - E_j A_j \varepsilon_i W_{ixx} = 0. \tag{7}$$

$$m_i U_{itt} - E_j A_j \varepsilon_{ix} = 0. \tag{8}$$

$$M_1 \ddot{U}_{CR} - M_1 g + T_1\left(L_1\right) + E_1 A_1\left(\varepsilon_1\right)\Big|_{x=L_1} - T_2\left(0\right) - E_2 A_2\left(\varepsilon_2\right)\Big|_{x=0} = 0. \tag{9}$$

$$M_2 \ddot{U}_{CS} - M_2 g + T_2\left(L_2\right) + E_2 A_2\left(\varepsilon_2\right)\Big|_{x=L_2} + T_3\left(L_3\right) + E_2 A_2\left(\varepsilon_3\right)\Big|_{x=L_3} = 0. \tag{10}$$

$$M_3 \ddot{U}_{CW} - M_3 g + T_4\left(L_4\right) + E_4 A_4\left(\varepsilon_4\right)\Big|_{x=L_4} - T_3\left(0\right) - E_2 A_2\left(\varepsilon_3\right)\Big|_{x=0} = 0. \tag{11}$$

where $\left(\ \right)_t \equiv \frac{\partial(\ )}{\partial t}$ and an overdot denotes the derivative with respect to time.

According to [3], in high rise buildings the bending motion frequencies $\Omega_v$ and $\Omega_w$ are much smaller than the longitudinal frequencies of the ropes, and we can assume that no interaction will take place between the lateral modes and the longitudinal modes of the ropes. As a result, the longitudinal inertia of all ropes can be neglected in Eq. (8) so that the model is reduced to two equations for each section of the suspension and compensating rope, respectively.

The boundary conditions in the lateral in-plane direction are defined as

$$V_1(0,t) = \xi_0(t). \quad V_1(L_1,t) = \xi_1(t). \tag{12}$$

$$V_2(0,t) = \xi_2(t). \quad V_2(L_2,t) = 0. \tag{13}$$

$$V_3(0,t)=\xi_3(t).\quad V_3(L_3,t)=0. \tag{14}$$

$$V_4(0,t)=\xi_5(t).\quad V_4(L_4,t)=\xi_4(t). \tag{15}$$

Where $\xi_0(t)$, $\xi_1(t)$, $\xi_2(t)$, $\xi_3(t)$, $\xi_4(t)$, and $\xi_5(t)$ represent the lateral displacements of the structure corresponding to the top of the structure and to the position of the car and counterweight (see Fig. 1). Similarly, the lateral out-plane displacements at the boundaries can be defined in a similar way. In order to accommodate the excitation in the equations of motion Eq. 6 and Eq. 7 the overall lateral in-plane displacements of each rope is expressed as

$$V_1(x_1,t)=\bar{V}_1(x_1,t)+\left(1+(\psi_1-1)\left(\frac{x_1}{L_1}\right)\right)C_v(t). \qquad 0<x_1<L_1. \tag{16}$$

$$V_2(x_2,t)=\bar{V}_2(x_2,t)+\left(1-\frac{x_2}{L_2}\right)\psi_2 C_v(t). \qquad 0<x_2<L_2. \tag{17}$$

$$V_3(x_3,t)=\bar{V}_3(x_3,t)+\left(1-\frac{x_3}{L_3}\right)\psi_3 C_v(t). \qquad 0<x_3<L_3. \tag{18}$$

$$V_4(x_4,t)=\bar{V}_4(x_4,t)+\left(\psi_5+(\psi_4-\psi_5)\left(\frac{x_4}{L_4}\right)\right)C_v(t). \qquad 0<x_4<L_4. \tag{19}$$

where $\bar{V}_i(x_i,t)$ are the displacements of the rope relative to the configuration each rope when it is stretched by the structure motion. Furthermore, $\psi_1$, $\psi_2$,$\psi_3$,$\psi_4$, and $\psi_5$ are the deformations obtained from the shape function $\Psi(z)$ which is assumed to be related to the fundamental mode of the high rise building and is approximated by a cubic polynomial as follows:

$$\psi_1=3\left(1-\frac{L_1}{h_0}\right)^2-2\left(1-\frac{L_1}{h_0}\right)^3. \tag{20}$$

$$\psi_2=3\left(\frac{L_2-b_1}{h_0}\right)^2-2\left(\frac{L_1-b_1}{h_0}\right)^3. \tag{21}$$

$$\psi_3=3\left(\frac{L_3-b_1}{h_0}\right)^2-2\left(\frac{L_3-b_1}{h_0}\right)^3. \tag{22}$$

$$\psi_4=3\left(1-\frac{L_4-b_2}{h_0}\right)^2-2\left(1-\frac{L_4-b_2}{h_0}\right)^3. \tag{23}$$

$$\psi_5=3\left(1-\frac{b_2}{h_0}\right)^2-2\left(1-\frac{b_2}{h_0}\right)^3. \tag{24}$$

Similarly, the lateral out-plane displacements of each rope are expressed in the same way. Using the transformations from Eq. (16) to Eq. (19) in Eq. (6) for the lateral in-plane motion, an approximate solution to the nonlinear partial differential equation of motion is determined by using the Galerkin method with the following finite series:

$$\bar{V}_i(x_i,t)=\sum_{r=1}^{N}\phi_{ir}(x_i)q_{ir}(t). \tag{25}$$

$$\bar{W}_i(x_i,t)=\sum_{r=1}^{N}\phi_{ir}(x_i)\mathrm{z}_{ir}(t). \tag{26}$$

where $\phi_{ir}(x_i) = \sin\left(\frac{n\pi}{L_i} x_i\right)$; $r = 1, 2, 3, ..., N$; with N denoting the number of modes, are the natural vibration modes of the corresponding $i^{th}$ rope and $q_{ir}(t)$ and $z_{ir}(t)$; $r = 1, 2, ..., N$ represent the lateral in-plane and lateral out of plane modal displacements, respectively.
These results in the following set of 4xN ordinary differential equations

$$\ddot{\mathrm{q}}_{ir}(t) + 2\zeta_{ir}\omega_{ir}\dot{\mathrm{q}}_{ir}(t) + \sum_{p=1}^{N} \bar{K}_{irp}\,\mathrm{q}_{ip}(t) = \bar{f}_{ir}^{\,q} + N_{ir}\,\mathrm{q}_{ir}(t). \tag{27}$$

$$\ddot{z}_{ir}(t) + 2\zeta_{ir}\omega_{ir}\dot{z}_{ir}(t) + \sum_{p=1}^{N} \bar{K}_{irp} z_{ip}(t) = \bar{f}_{ir}^{\,z} + N_{ir} z_{ir}(t). \tag{28}$$

The modal damping represented by the ratios $\zeta_{ir}$ and the undamped time varying natural frequencies of the element $\omega_{ir}$. The $\bar{K}_{irp}$ is the stiffness matrix, $\bar{f}_{ir}^{\,q}$ and $\bar{f}_{ir}^{\,z}$ represent the excitation force terms and $N_{ir}$ are the nonlinear terms.

Similarly, the equations of motion for the car, compensating sheave, and counterweight from (9) to (11) are transformed into the modal coordinates using the transformation

$$\vec{U} = [Y]\vec{S} \tag{29}$$

where $\vec{U} = \begin{bmatrix} U_{CR} & U_{CS} & U_{CW} \end{bmatrix}^T$ and $\vec{S} = \begin{bmatrix} S_{CR} & S_{CS} & S_{CW} \end{bmatrix}^T$ is a vector of modal-coordinates corresponding to the system comprising the car, compensating sheave, and counterweight, respectively. If [*Y*] is the mass-normalized mode shape matrix, the following set of equations describing the vertical response of the car, compensating sheave and counterweight: in terms of the modal parameters

$$\ddot{S}_{CR}(t) + 2\zeta_{CR}\omega_{CR}\dot{S}_{CR}(t) + \omega_{CR}^2 S_{CR}(t) = \left(\vec{Y}^{(1)}\right)^T \left(\vec{F} + \vec{\eta}\right). \tag{30}$$

$$\ddot{S}_{CS}(t) + 2\zeta_{CS}\omega_{CS}\dot{S}_{CS}(t) + \omega_{CS}^2 S_{CS}(t) = \left(\vec{Y}^{(2)}\right)^T \left(\vec{F} + \vec{\eta}\right). \tag{31}$$

$$\ddot{S}_{CW}(t) + 2\zeta_{CW}\omega_{CW}\dot{S}_{CW}(t) + \omega_{CW}^2 S_{CW}(t) = \left(\vec{Y}^{(3)}\right)^T \left(\vec{F} + \vec{\eta}\right). \tag{32}$$

where $\zeta_{CR}$, $\zeta_{CS}$, $\zeta_{CW}$ and $\omega_{CR}$, $\omega_{CS}$, $\omega_{CW}$ denote the modal damping ratios and the natural frequencies of the car, compensating sheave and counterweight, respectively, and $\vec{Y}^{(i)}$ is the *i*th mode shape vector. The $\vec{F} = \begin{bmatrix} \bar{F}_{CR} \\ \bar{F}_{CS} \\ \bar{F}_{CW} \end{bmatrix}$ is the excitation vector, and the $\vec{\eta} = \begin{bmatrix} \eta_{CR} \\ \eta_{CS} \\ \eta_{CW} \end{bmatrix}$ is a vector with components representing the nonlinear couplings with the lateral motions of the ropes.

## CASE STUDY

The dynamic performance of an elevator system comprising seven ($n_1 = 7$) steel wire suspension ropes and four ($n_2 = 4$) steel wire compensating ropes of mass per unit length $m_1 = 0.723$ kg/m and $m_2 = 1.1$ kg/m, having modulus of elasticity $E = 54535$ N/mm$^2$ and nominal diameters $d_1 = 13$ mm and $d_2 = 16$ mm, respectively. The modal damping ratios for the ropes are assumed as 0.3% across all modes and 10% for the lumped mass across all modes. The height measured from the ground

floor level to the center of the traction sheave is $h_0 = 88.875$ m, the car and counterweight height is $h_{cw} = h_{car} = 4.00\,\text{m}$, travel height $h_{trav} = 80.70\,\text{m}$, the car mass with full load is $M_1 = 4400\,\text{kg}$, the mass of the compensating sheave is $M_2 = 600\,\text{kg}$, and the mass of the counterweight is $M_3 = 3600\,\text{kg}$. The elevator car is positioned at the top landing level. The height measured from the bottom landing level to the center of the compensating sheave is given as $b_1 = 2.02\,\text{m}$ and the height from center of the traction sheave to the center of the diverter pulley is $b_2 = 0.80\,\text{m}$. The high rise building is excited by the wind harmonically in the lateral in-plane direction with a frequency of $\Omega_v = 1.220\,\text{rad/s}$ (0.1941 Hz), amplitude of $A_v = 0.07$ m and in the lateral out of plane direction with a frequency of $\Omega_w = 0.314\,\text{rad/s}$ (0.05 Hz) and amplitude of $A_w = 0.005\,\text{m}$. Table 1 shows the frequencies of the first 4 modes of the ropes.

| Rope No. # | 1 Mode [Hz] | 2 Mode [Hz] | 3 Mode [Hz] | 4 Mode [Hz] |
|---|---|---|---|---|
| 1 | 11.88 | 23.76 | 35.63 | 47.51 |
| 2 | 0.19 | 0.39 | 0.58 | 0.80 |
| 3 | 6.45 | 12.89 | 19.35 | 25.80 |
| 4 | 0.53 | 1.06 | 1.60 | 2.13 |

Table 1. The first 4 natural frequencies of the ropes.

The variation of the first four natural frequencies of the compensating ropes at the car side against the position of the elevator car in the hoistway measured from the bottom landing level is shown in Fig. 2. The horizontal lines represent the lateral in-plane and the lateral out of plane frequencies of the building.

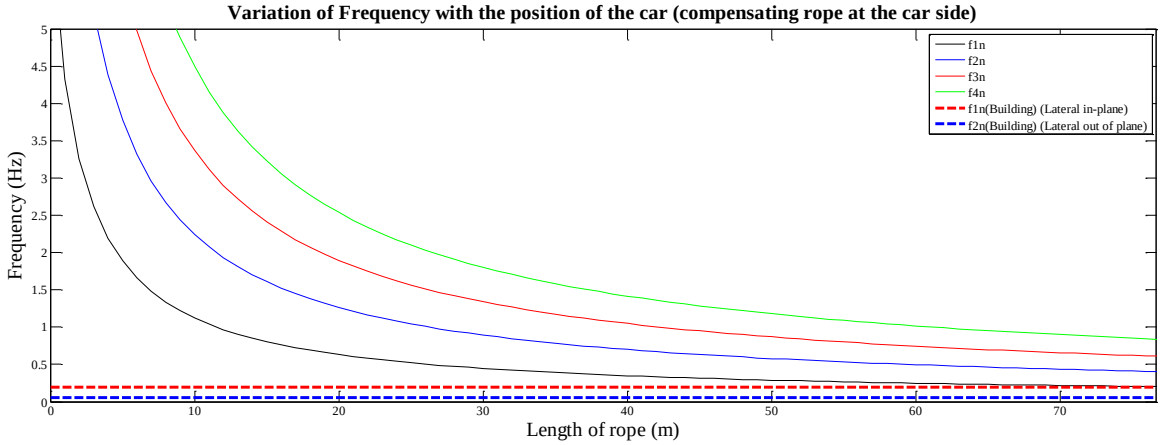


Figure 2. Variation of the first four natural frequencies of the compensating ropes at the car side.

The trajectory of the building recorded at the machine room level over time interval of 60 seconds is shown in Fig. 3.

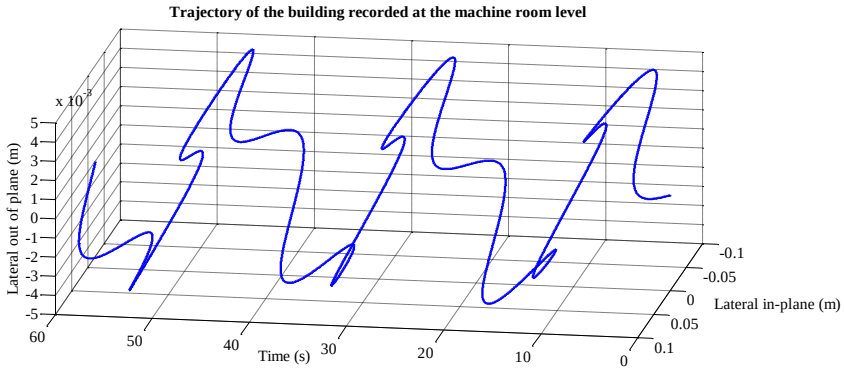


Figure 3. Trajectory of the building recorded at the machine room level.

The mode shapes corresponding to the vertical vibrations of the car, compensating sheave and counterweight are shown in Fig. 4 (a), (b) and (c), respectively. In the first mode (2.58 Hz) the compensating sheave and counterweight have greater displacements than the car and they are in phase. The second mode (8.54 Hz) is dominated by the car motion with the displacements of the compensating sheave and counterweight being almost zero. In the third mode (33 Hz) the car motions are negligible and the compensating sheave vibrations are dominant. The displacements of the compensating sheave and counterweight are out of phase.

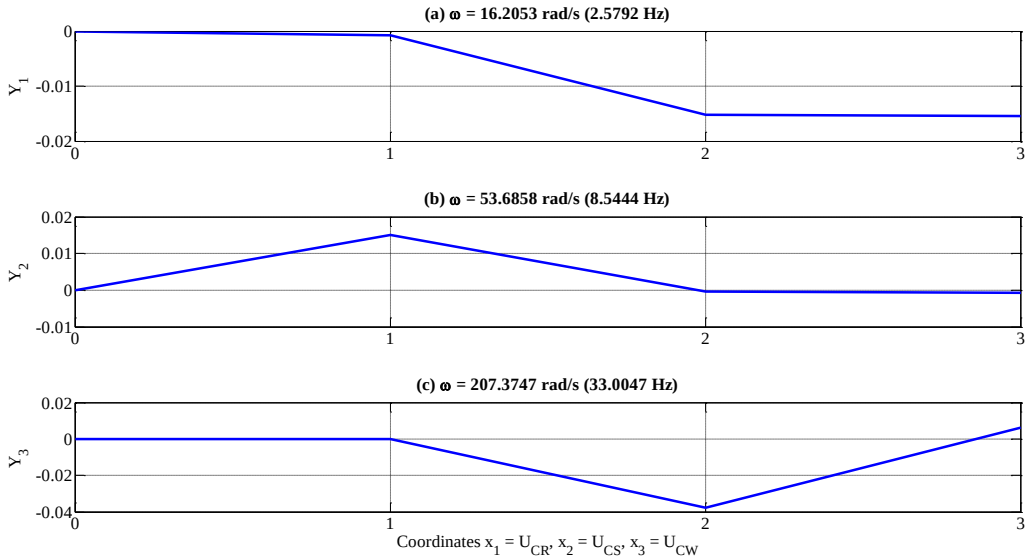


Figure 4. The mode shape displacements of the car, compensating sheave and counterweight.

In order to predict the dynamic response of the ropes and discrete masses, the equations of motion Eqs. (27), (28), (30), (31), and (32) are integrated numerically using an explicit Runge-Kutta fourth- and fifth-order furmula. The numerical procedure is started from the initial instant $t_0 = 0\,\mathrm{s}$ until $t_f = 600\,\mathrm{s}$.

The lateral in-plane and the lateral out of plane displacements versus time are shown in Fig. 5 (a) and (b), respectively. The displacements in the lateral out of plane directions are very small when the simulation starts. However, they are increasing with time and whirling motions of the rope result as shown in Fig. 6.

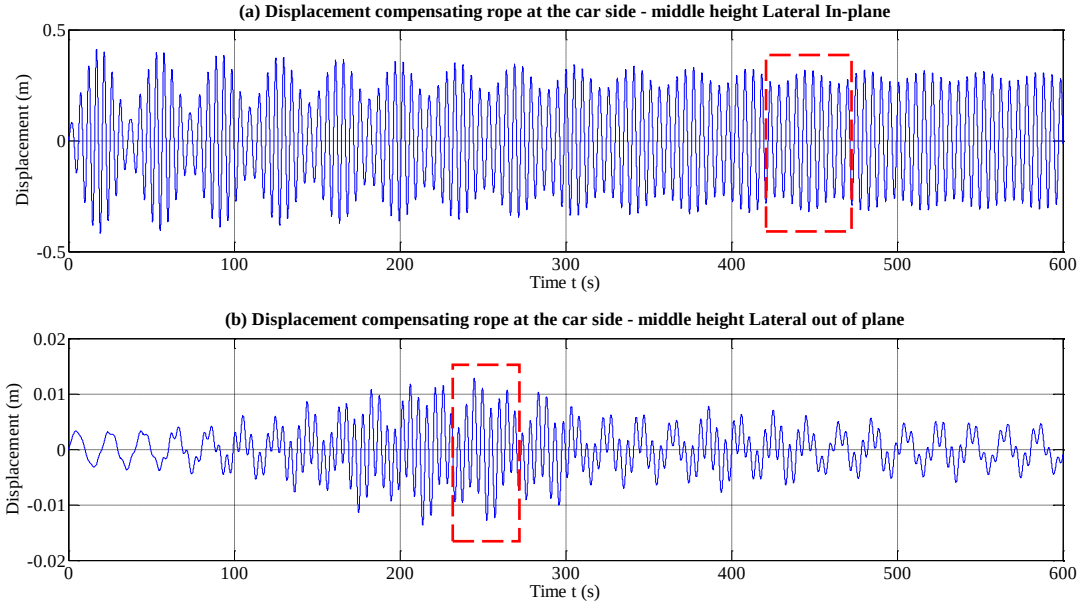


Figure 5. The mid-span displacements of the compensating rope at the car side with respect to time.

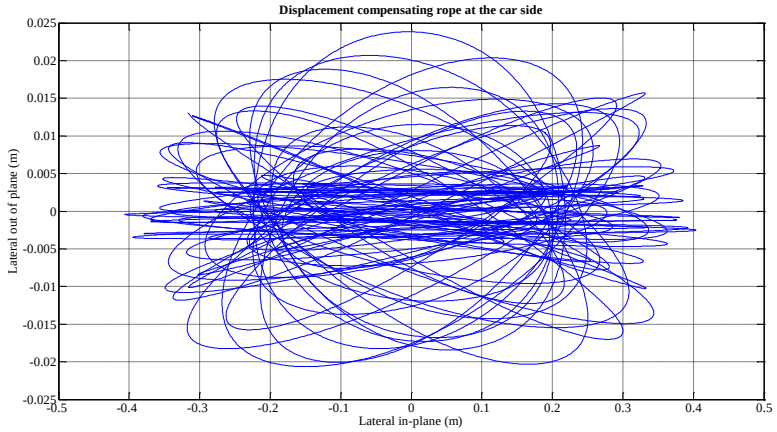


Figure 6. Lateral displacement of the compensating ropes at the car side.

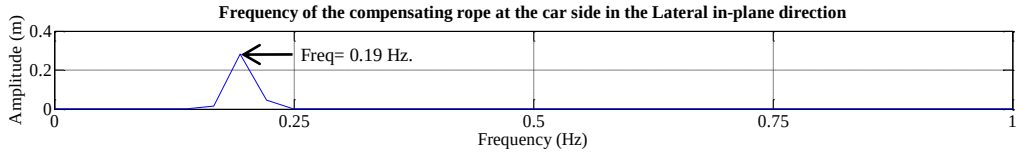


Figure 7. Frequency of the compensating rope at the car side in the Lateral in-plane.

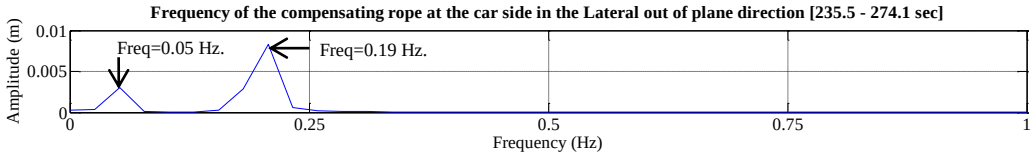


Figure 8. Frequency of the compensating rope at the car side in the Lateral out of plane.

The displacement time records of the car, compensating sheave, and counterweight are shown in Fig. 9 (a), (b), and (c), respectively, with the corresponding frequency spectra plotted in Fig. 9 (d), (e), and (f), respectively. It is evident that the dominant frequency is twice the frequency of the in-plane excitation (0.39 Hz). The FFT frequency spectra of the lateral in-plane over a time span of 428.8 – 464.9 s and for the lateral out of plane directions over a time span of 235.5 – 274.1 s are

shown in Fig. 7 and 8, respectively. It is evident that the dominant frequency is the frequency of the in-plane direction (0.19 Hz).

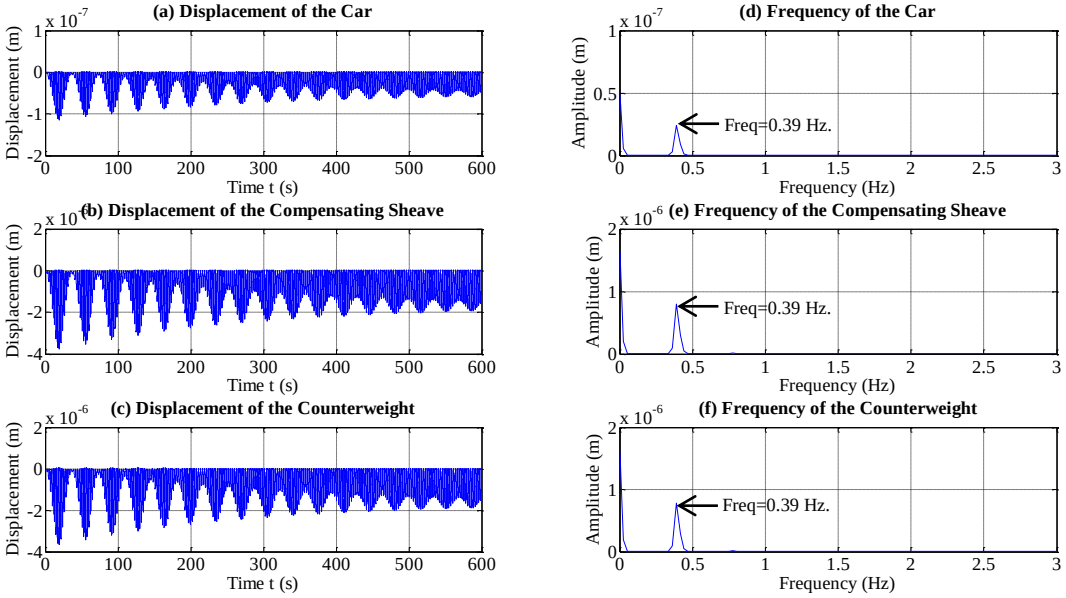


Figure 9. Displacements and FFT frequency spectra of the car, compensating sheave, and counterweight.

## CONCLUSIONS

The equations of motion of a stationary elevator system comprising an elevator car, compensating sheave, counterweight, with suspension and compensating ropes excited by the high rise building motions are derived in this paper. These equations accommodate the nonlinear effects of the rope stretching in the lateral in-plane and the lateral out of plane directions. This model is used to predict the response of the system. Numerical simulation results show that at the resonance conditions the transfer of energy from the lateral in-plane mode to the lateral out of plane mode takes place. While the motions of the structure are small, the rope is experiencing large lateral whirling motions. If the response of the ropes continue to grow impact phenomena in the hoistway might occur which may lead to excessive vibrations of the car and damage to the system components.

## ACKNOWLEDGMENTS

Support received from ThyssenKrupp Elevator AG for the research work reported in this paper is gratefully acknowledged.

## REFERENCES

[1] Salamaliki-Simpson R., Kaczmarczyk S., Picton P. and Turner S. (2006) Non-Linear Modal Interactions in a Suspension Rope System with Time-Varying Length. *Applied Mechanics and Materials.* **5-6** (2006), 217-224.

[2] Kaczmarczyk S. (2012) The Nonstationary, nonlinear dynamic interactions in slender continua deployed in high-rise vertical transportation systems in the modern built environment. *Modern Practice in Stress and Vibration Analysis 2012.* Journal of Physics: Conference Series **382.**

[3] Kaczmarczyk S. and Picton P. (2013) The prediction of Nonlinear Responses and Active Stiffness Control of Moving Slender Continua Subjected to Dynamic Loadings in Vertical Host Structures. *International Journal of Acoustics and Vibration.* **18** (1), pp. 39 – 44.